Softening and Fracturing Process in Masonry Arches

(Processo di fessurazione e assestamento negli archi lapidei)

ALBERTO CARPINTERI, ANDREA CARPINTERI

Istituto di Scienza delle Costruzioni, Università di Bologna,
2 Viale Risorgimento, 40136 Bologna, Italy.

Abstract - The softening and fracturing process in shallow masonry arches is considered. Therefore a purely elastic constitutive law is assumed for the material, coupled with a fracturing crisis condition according to Fracture Mechanics concepts.
It is numerically verified how the cracks control the line of thrust, so that the statical behaviour of the structure is improved and the internal loadings are redistributed. It is then possible to define a parameter called "fracturing benefit".
Moreover the intermediate stage of structural damage is caught, which occurs during the loading process and immediately follows and precedes the situations relating to the traditional schemes of elastic and limit analysis.

Sommario - Si considera il problema dell'assestamento per fessurazione di archi elasto-softening ribassati. Si assume quindi una legge costitutiva del materiale puramente elastica, abbinata ad una condizione di crisi per fessurazione nel senso della Meccanica della Frattura.
Si verifica numericamente come la presenza di fessure controlli l'andamento della curva delle pressioni, in modo da migliorare il comportamento statico della struttura e da ridistribuirne le sollecitazioni interne, e si perviene alla definizione di un parametro detto "beneficio per fessurazione".
Si coglie inoltre quella fase intermedia di danneggiamento della struttura, che si verifica durante il processo di carico e che immediatamente segue e precede le situazioni relative agli schemi tradizionali di calcolo elastico e a rottura.

1. INTRODUCTION.

The analysis of masonry structures constitutes a topic of growing interest, especially in relation to the recent seismical events, which have caused damage to and fracturing of several ancient constructions in Italy.

As regards arch-structures, and more generally vault-structures, the traditional schemes of elastic and limit analysis [1], even if scientifically settled, often leave the structural engineer quite embarrassed. Namely, while the elastic analysis considers the structure completely in compression and then verifies the line of thrust does not go out of the inertial core, the limit analysis is restricted to consider the material as completely incoherent (not traction bearing) and to verify the line of thrust does not go out of the volume of the arch itself. Therefore both these structural analysis schemes do not catch that intermediate stage of damaging, which occurs during the loading process of the structure and immediately follows and precedes the situations relating to the above-mentioned schemes. That is, while the elastic analysis describes the structure up to the rise of the first non-linearities, the limit analysis takes into consideration only the last situation prior to the final collapse.

This need for a more sophisticated computational technique, considering the real constitutive laws of the material and allowing the fracturing stage - intermediate between elastic behaviour and final collapse - to be investigated, has been recently pointed out in [2], where a computational procedure founded on the Minimum Complementary Energy Principle has been proposed. In that context an elastic-incoherent material (Fig. 1-a) and an elastic-brittle material (Fig. 1-b) have been considered. Probably a better schematization, for masonry and more generally for aggregative materials, would be an elastic-softening material (Fig. 1-c) [3].

On the other hand, as Hillerborg [4] has recently shown, considering an elastic-softening constitutive law for the material is equivalent to considering a simply elastic constitutive law, coupled with a fracturing crisis condition according to Fracture Mechanics concepts. Therefore, while the total stress relaxation can be described only by the constitutive law in the former case, in the latter it is realized by the crack propagation mechanism, with evident computational advantages.

It is a traditional belief that cracks in elastic-softening arch-structures control the line of thrust, so that the statical behaviour is improved and the internal loadings are redistributed. The same thing qualitatively happens in elastic-plastic framed structures, with the formation of plastic hinges. The present preliminary investigation has been developed for pointing out such positive fracturing effects, and the problem of softening and fracturing process in shallow masonry arches has been examined. Then a discrete model of the structure has been assumed, constituted by beam finite elements, and a monotonic step by step loading process has been considered. For each loading increment the axial force and the bending moment at the ends of every beam element have been computed. Based on such values, a check against crushing and tensile crises has been performed. When a crushing crisis occurs, such a crisis is considered as definitive for the structure, while in the case of a tensile crisis occuring the routine simulates a crack formation, introducing an elastic hinge of suitable stiffness. The crack depth is determined by means of Fracture Mechanics concepts: it stabilizes at a value, which is a function of the axial force, of its eccentricity and of the geometrical and mechanical features of the cross-section.

Knowing the crack depth, it is possible to compute the rotational stiffness of the crack simulating elastic hinge; then the local stiffness matrix of the cracked element is revised and eventually the global matrix of the arch. The procedure takes into consideration even the possibility of a partial or total

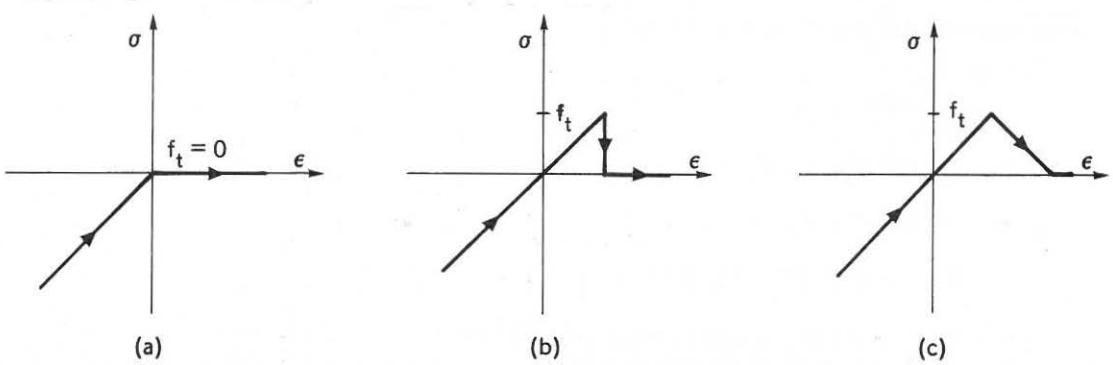

Fig. 1 - Constitutive laws for masonry: (a) elastic-incoherent; (b) elastic-brittle; (c) elastic-softening.

crack closure, during loading increments following that of crack formation.

As an illustrative application of the above mentioned procedure a family of shallow parabolic arches, with constant span and variable rise, uniformly loaded along the span, will be numerically examined.

2. MECHANISMS OF CRACK OPENING AND CLOSURE.

As has already been anticipated in the Introduction, the elastic-softening material will be replaced by a purely elastic material with the possibility of crack formation and extension. Such an hypothesis is valid only when the structure is sufficiently large so that stress profiles, close to those obtained from Linear Elastic Fracture Mechanics [3][5], can develop at middle distances from the crack tip.

As damage parameter, the relative crack depth $\xi = a/b$ will be considered (Fig. 2-a) and, as loading parameter, the stress-intensity factor K_I (Fig. 2-b), which is an amplification factor of the stress field when the loadings are only symmetrical (e.g. axial force and bending moment). The shear force will then be ignored.

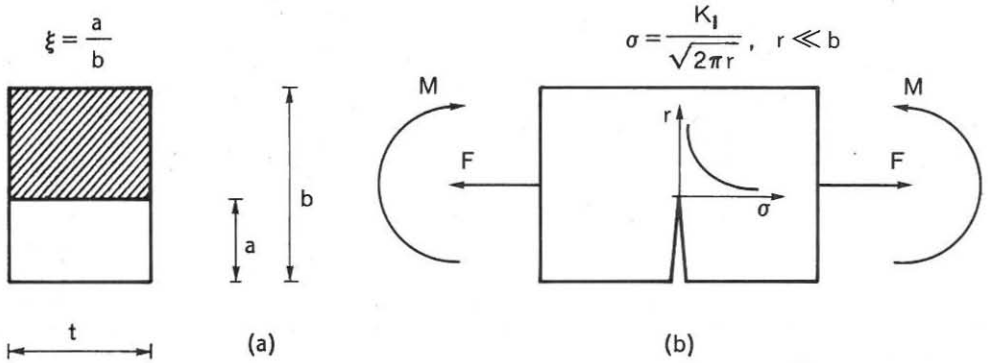

Fig. 2 - Cracked beam element: (a) damage parameter ξ; (b) loading parameter K_I.

It is interesting to recall the energetic meaning of K_{IC}: the square of such a parameter — neglecting a factor of proportionality — namely represents the elastic energy released by the system in a virtual unit crack extension. When K_I achieves its critical value K_{IC}, it means that such an extension from virtual becomes real, since the released energy in an elementary crack extension is sufficient to provide the surface energy of the new topology.

As is well-known, a bending moment induces a stress-intensity factor at the crack tip equal to (Fig. 2):

$$K_I^{(M)} = \frac{M}{b^{3/2} t} Y_M(\xi), \tag{1}$$

while a tensile axial force F induces the factor:

$$K_I^{(F)} = \frac{F}{b^{1/2} t} Y_F(\xi), \tag{2}$$

where the functions Y_M and Y_F, for $0 \leqslant \xi \leqslant 0.7$, are [6]:

$$Y_M(\xi) = 6 \times (1.99\,\xi^{1/2} - 2.47\,\xi^{3/2} + 12.97\,\xi^{5/2} - 23.17\,\xi^{7/2} + 24.80\,\xi^{9/2}),$$

$$Y_F(\xi) = 1.99\,\xi^{1/2} - 0.41\,\xi^{3/2} + 18.70\,\xi^{5/2} - 38.48\,\xi^{7/2} + 53.85\,\xi^{9/2}.$$

When the axial force F is a compression and the bending moment M tends to open the crack, as happens at the cross-sections of the arch-structures, the total stress-intensity factor can be obtained ap-

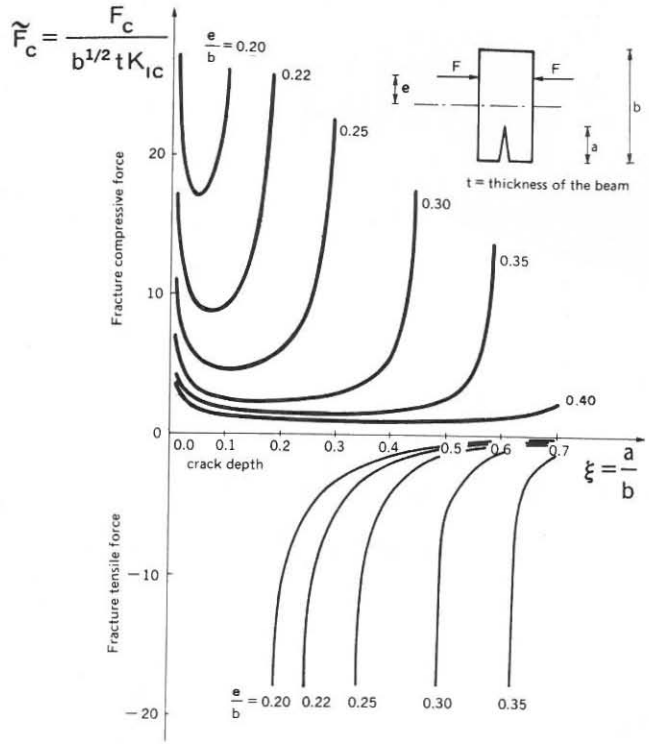

Fig. 3 - Stability of fracturing process in an axially loaded beam.

plying the superposition principle:

$$K_I = K_I^{(M)} - K_I^{(F)} = \frac{F}{b^{1/2} t}\left[\frac{e}{b} Y_M(\xi) - Y_F(\xi)\right], \tag{3}$$

where e indicates the eccentricity of the equivalent eccentric axial force.
From the critical condition $K_I = K_{IC}$, the dimensionless axial force of crack extension can be obtained, as a function of the crack depth ξ and varying the relative eccentricity e/b of the load [7]:

$$\tilde{F}_c = \frac{F_c}{b^{1/2} t K_{IC}} = \frac{1}{\frac{e}{b} Y_M(\xi) - Y_F(\xi)} . \tag{4}$$

The curves of Fig. 3 graphically represent expression (4) and show how — fixed the eccentricity e/b — fracturing achieves a stable stage only after presenting an unstable one. If the load F has not the possibility to follow the unstable descending branch of the curve e/b = constant, in a "strain-softening" unloading process, fracturing will have catastrophical behaviour [8] and the representative point will horizontally advance in the diagram of Fig. 3 to meet again the curve e/b = constant on its stable branch. On the other hand the load relaxation possibility, and then the more or less catastrophical fracturing behaviour, depends — as will be shown afterwards — on the geometrical and mechanical structural features, and especially on the degree of redundancy and on the sizes (scale effect).

Then it is important to consider that, for each relative crack depth ξ, a relative eccentricity e/b exists, under which crack closes again, at least partially. From the closing condition $K_I = 0$:

$$\frac{e}{b} = Y_F(\xi) / Y_M(\xi) . \tag{5}$$

The curve of Fig. 4 graphically represents expression (5). The points under the curve represent cracks

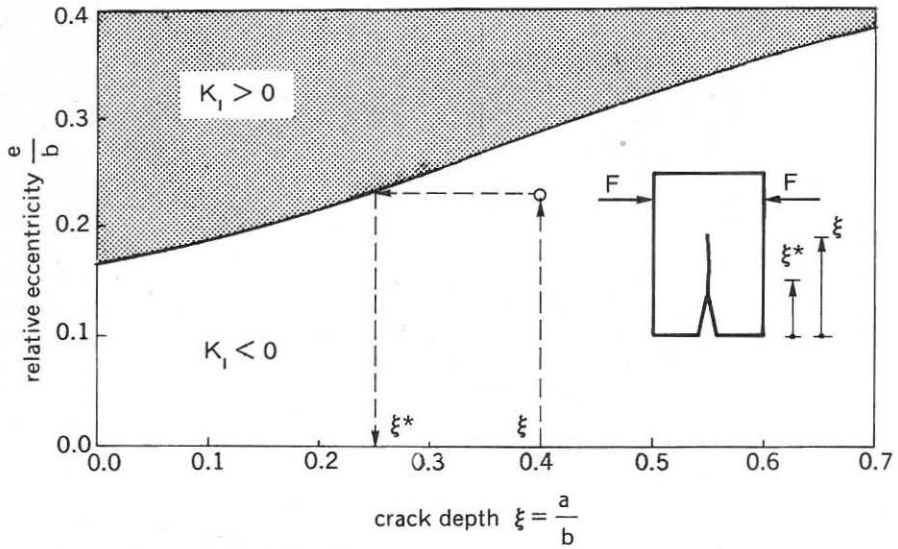

Fig. 4 - Curve of crack closure.

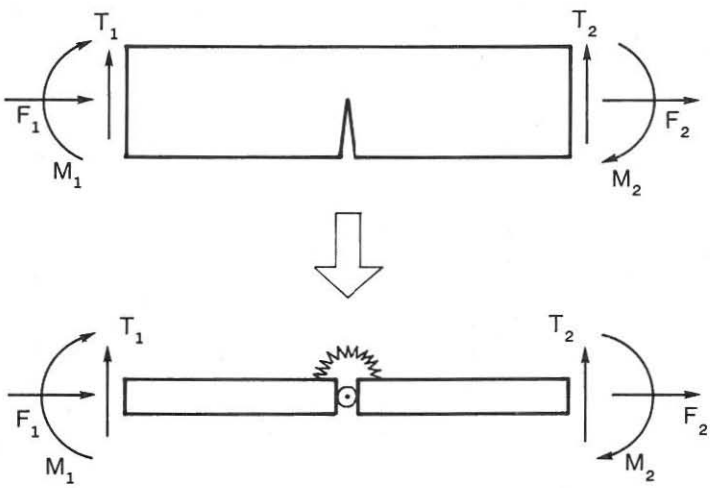

Fig. 5 - Cracked beam finite element.

and loading conditions for which $K_I < 0$. Afterwards numerical examples will be shown where the crack will tend to close again; a fictitious crack depth ξ^* (lower than the real depth ξ) will be defined, obtainable from condition (5) (Fig. 4).

The stiffness loss of a cracked beam cross-section is eventually considered. Namely, while an uncracked cross-section of a beam element carries out an internal action of perfectly fixed joint, a cracked cross-section carries out an internal action of elasticly fixed joint, with rotational stiffness (Fig. 2-a):

$$W = \frac{b^2 t E}{\int_0^{\xi} Y_M^2(\xi)\, d\xi} , \qquad (6)$$

where E is the Young's modulus of the material. Such a stiffness can be obtained by an energetic balance between elastic work and fracture work [9].

The stiffness matrix of the cracked beam finite element (Fig. 5), is modified only in the four

rotational terms, as follows:

	u_1	v_1	φ_1	u_2	v_2	φ_2
F_1	$\frac{EA}{\ell}$	0	0	$-\frac{EA}{\ell}$	0	0
T_1		$12\frac{EI}{\ell^3}$	$-6\frac{EI}{\ell^2}$	0	$-12\frac{EI}{\ell^3}$	$-6\frac{EI}{\ell^2}$
M_1			$\frac{EI(3EI+4\ell W)}{\ell(EI+\ell W)}$	0	$6\frac{EI}{\ell^2}$	$\frac{EI(3EI+2\ell W)}{\ell(EI+\ell W)}$
F_2				$\frac{EA}{\ell}$	0	0
T_2		SYMMETRICAL			$12\frac{EI}{\ell^3}$	$6\frac{EI}{\ell^2}$
M_2						$\frac{EI(3EI+4\ell W)}{\ell(EI+\ell W)}$

(7)

where A and I indicate area and moment of inertia of the cross-section, and ℓ is the length of the beam finite element.

3. NUMERICAL EXAMPLES.

As a model structure, to which to apply the concepts introduced in the preceding section, consider the shallow arch of Fig. 6, with constant span L = 50 m and variable rise h, rectangular cross-section of thickness t = 40 cm and width b = 80 cm, uniformly loaded along the span. Then hypothesize the arch as constituted in masonry, with tensile strength f_t = 30 kg cm^{-2}, compression strength f_c = 500 kg cm^{-2}, and a critical value K_{IC} of the stress-intensity factor equal to 50 or 100 kg cm$^{-3/2}$.

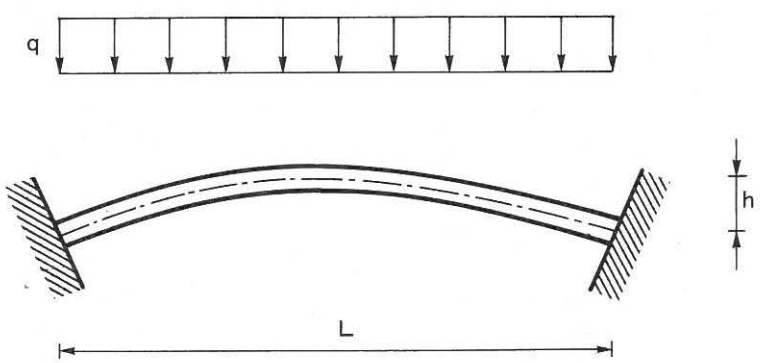

Fig. 6 - Shallow arch—structure.

As a first case, let it be h/L = 1/20 and K_{IC} = 100 kg cm$^{-3/2}$. For q = 42.67 kg cm^{-1} in the boundary finite elements the tensile strength f_t and the compressive stress — 342 kg cm^{-2} < f_c are reached. Then the routine computes the corresponding dimensionless axial force $\tilde{F}_c$ = 13.95 and the eccentricity e/b = 0.20. The diagram of Fig. 3 shows how, for such values, the crack formation is not possible yet. It is necessary to increase the load q up to 51.86 kg cm^{-1}, so that the couple of values $\tilde{F}_c$ = 16.96 and e/b = 0.20 can be achieved and a stable crack of depth ξ = 0.05 forms (minimum of the curve e/b = 0.20 of Fig. 3). At this point the routine verifies that other cracks can not form in the structure, besides those of the boundary elements.

At the following step, an elastic hinge is introduced in the cracked elements, i.e. the original structure is replaced by another one of lower global stiffness, and the above described procedure is repeated, maintaining q = 51.86 kg cm^{-1}: the crack depth remains 0.05 b. Then the load q is increased to 60 kg cm^{-1}, obtaining $\tilde{F}_c$ = 19.62 and e/b = 0.20, and then ξ = 0.08.

At the third step, with ξ = 0.08 and q = 60 kg cm^{-1}, the preceding results are obtained again and then the load is increased to q = 62.38 kg cm^{-1}, achieving the crushing in the boundary elements (— 500 kg cm^{-2}). Such a collapse is supposed to be definitive.

As a second case, let it be h/L = 1/20 again and assume a lower fracture resistance K_{IC} = 50 kg cm$^{-3/2}$. In this case, for q = 42.67 kg cm^{-1}, at the fixed ends one has $\tilde{F}_c$ = 27.90 and e/b = 0.20, from which ξ = 0.105. The crack formation is allowed by the lower value K_{IC}, which has now been chosen. At the second step, with ξ = 0.105 and q = 42.67 kg cm^{-1}, one has $\tilde{F}_c$ = 27.90 and e/b = 0.198 and then a depth ξ < 0.105. Then the routine resorts to the curve of closure (Fig. 4), which, for e/b = 0.198, gives ξ^* = 0.130 > 0.105. Thus the routine chooses the value ξ = 0.105. Then the load is increased up to q = 45 kg cm^{-1} and the crack stabilizes for ξ = 0.110.

At the third step (ξ = 0.110, q = 45 kg cm^{-1}) ξ = 0.110 results again, and the load is increased to 60 kg cm^{-1}. The crack stabilizes for ξ = 0.120.

At the fourth step, an increment of q to 62.38 kg cm^{-1} produces the final crushing collapse, with a very slight delay compared to the case of uncracked structure.

As a third case, let it be h/L = 1/30 and K_{IC} = 100 kg cm$^{-3/2}$. For q = 7.71 kg cm^{-1}, at the fixed ends, one has $\tilde{F}_c$ = 3.36 and e/b = 0.30, from which ξ = 0.335. At the second step, with ξ=0.335, one obtains $\tilde{F}_c$ = 3.40 and e/b = 0.28, from which the new depth is ξ = 0.225. Then it is necessary to apply the curve of closure (Fig. 4), which gives ξ^* = 0.385. Therefore the routine maintaines ξ = 0.335. For q = 17 kg cm^{-1}, one obtains $\tilde{F}_c$ = 7.51 and e/b = 0.28, and then ξ = 0.350.

At the third step, with q = 38.46 kg cm^{-1}, the crushing collapse occurs. Observe how the load of definitive collapse is substantially higher than the load of first fracturing (Table 1).

Tab. 1 - Loads of first fracture q_f and final collapse q_c (L = 50m).

h/L	K_{IC}	q_f/q_0	q_c/q_0
1/20	100	0.83	1.00
1/20	50	0.68	1.00
1/30	100	0.21	1.05
1/30	50	0.21	1.05
1/40	100	0.15	1.11
1/40	50	0.15	0.15

As a fourth case, consider h/L = 1/30 and K_{IC} = 50 kg cm$^{-3/2}$. For q = 7.71 kg cm^{-1} one has ξ = 0.40 at the ends of the arch. At the second step, one obtains ξ = 0.26 and, appying the curve of crack closure, from ξ = 0.40 and e/b = 0.26 it follows a real closure: ξ^* = 0.35.
At the third step, $\tilde{F}_c$ = 6.81 and e/b = 0.27 provide ξ = 0.30, while the curve of closure gives ξ^* = 0.38; therefore the crack stabilizes at ξ = 0.35. Increasing the load — q = 30 kg cm^{-1} — it follows ξ = 0.353. Then, for q = 38.53 kg cm^{-1}, the crushing collapse occurs. The uncracked structure would crush with q = 36.71 kg cm^{-1}; therefore the fracturing process has a "beneficial effect" on the load of collapse (Table 1).

As a fifth case, consider h/L = 1/40 and K_{IC} = 100 kg cm$^{-3/2}$. For q = 3.77 kg cm^{-1} one has ξ = 0.67 at the arch ends. At the second step the crack closes: ξ^* = 0.223. At the following steps the crack presents an oscillating behaviour: ξ = 0.58; ξ^* = 0.40; ξ = 0.45. Eventually, for q = 28.71 kg cm^{-1}, the crushing collapse occurs. The same collapse would occur for q = 25.82 kg cm^{-1} in the uncracked structure (Table 1).

As a sixth and last case, consider h/L = 1/40 and K_{IC} = 50 kg cm$^{-3/2}$. Already for q = 3.77 kg cm^{-1} it results $\xi > 0.7$ and then the fracture collapse comes before the crushing collapse; thus the fracturing benefit has no way of being observed (1).

In Table 1, for each rise h/L and each considered K_{IC} value, the load q_f of first fracturing and the load q_c of final collapse have been summarized; they have been normalized by the load of crushing q_0, related to the case in which the crack formation is not taken into consideration. The ratio q_c/q_0 can be defined "fracturing benefit" and is analogous to the "plastic benefit" of the limit analysis.

In table 2 the results have then been reported, concerning the case in which the sizes of the previous examples are multiplied by 10 (L = 500 m, t = 4 m, b = 8 m). It is possible to observe how two of the new computed ratios are lower than the corresponding ratios of Table 1. Therefore a scale effect is present; it means that the increase of the system size makes the system itself more brittle, independently of the constitutive law of the material [10] [11].

Tab. 2 - Loads of first fracture q_f and final collapse q_c (L = 500m).

h/L	K_{IC}	q_f/q_0	q_c/q_0
$\frac{1}{20}$	100	0.68	1.00
$\frac{1}{20}$	50	0.68	1.00
$\frac{1}{30}$	100	0.21	1.05
$\frac{1}{30}$	50	0.21	1.05
$\frac{1}{40}$	100	0.15	0.15
$\frac{1}{40}$	50	0.15	0.15

(1) When $\xi > 0.7$, a definitive fracture collapse is assumed.

ACKNOWLEDGMENTS.

The authors gratefully acknowledge the financial support of the Italian National Research Council (C.N.R.).

References

[1] V. FRANCIOSI: L'attrito nel calcolo a rottura delle murature — Giornale del Genio Civile, fasc. 7 - 8 - 9, pp. 215 - 234, 1980.

[2] A. BARATTA, M. VIGO and G. VOIELLO: Calcolo di archi in materiale non resistente a trazione mediante il principio del minimo lavoro complementare, "Consolidamento e Restauro Architettonico" — I Congresso Nazionale ASS.I.R.C.C O., Verona, 30 sept./3 oct. 1981.

[3] Z.P. BAŽANT: Instability, Ductility and Size Effect in Strain-Softening Concrete — Journal of the Engineering Mechanics Division, A.S.C.E., Vol. 102, No. EM2, pp. 331 - 344, 1976.

[4] A. HILLERBORG, M. MODEER and P.E. PETERSSON: Analysis of crack formation and crack growth in concrete by means of Fracture Mechanics and Finite Elements — Cement and Concrete Research, Vol. 6, pp. 773 - 782, 1976.

[5] A. CARPINTERI: Application of Fracture Mechanics to Concrete Structures — Journal of the Structural Division, A.S.C.E., April 1982.

[6] A. CARPINTERI: A Fracture Mechanics Model for Reinforced Concrete Collapse, "Advanced Mechanics of Reinforced Concrete" — IABSE Colloquium Final Report, Delft, 2/4 june 1981.

[7] A. CARPINTERI, A. DI TOMMASO and E. VIOLA: On the limit bearing capacity of cracked masonry walls (in Italian) — Proceedings 5th Congress of the Italian Association of Theoretical and Applied Mechanics (AIMETA), Palermo, 1980.

[8] R. THOM: Structural stability and morphogenesis — Benjamin, New York, 1975.

[9] A. CARPINTERI: Stiffness Loss and Fracture Resistance of a Cracked Beam with Circular Cross-Section — Internal Report n. 56 — I.S.C.B., 1981.

[10] A. CARPINTERI: Notch Sensitivity in Fracture Testing of Aggregative Materials — Engineering Fracture Mechanics, to appear.

[11] A. CARPINTERI: Static and energetic fracture parameters for rocks and concretes — Materials & Structures, R.I.L.E.M., Vol. 14, No. 81, pp. 151 - 162, 1981.